



Akt and p53 are potential mediators of reduced mammary tumor growth by Chloroquine and the mTOR inhibitor RAD001

Christian R. Loehberg^{a,*}, Pamela L. Strissel^a, Ralf Dittrich^a, Reiner Strick^a, Juergen Dittmer^b, Angela Dittmer^b, Ben Fabry^c, Willi A. Kalender^c, Thorsten Koch^c, David L. Wachter^d, Nicole Groh^a, Astrid Polier^a, Ina Brandt^a, Laura Lotz^a, Inge Hoffmann^a, Florentine Koppitz^a, Sonja Oeser^a, Andreas Mueller^a, Peter A. Fasching^a, Michael P. Lux^a, Matthias W. Beckmann^a, Michael G. Schrauder^a

^a Department of Obstetrics and Gynecology, University Hospital Erlangen, Universitaetsstr. 21-23, 91054 Erlangen, Germany

^b Department of Obstetrics and Gynecology, University Hospital Halle, Ernst-Grube-Str. 40, 06120 Halle (Saale), Germany

^c Center for Medical Physics and Technology, University of Erlangen-Nuremberg, Henkestrasse 91, 91052 Erlangen, Germany

^d Department of Pathology, University Hospital Erlangen, Krankenhausstr. 9, 91054 Erlangen, Germany

ARTICLE INFO

Article history:

Received 13 October 2011

Accepted 21 November 2011

Available online 28 November 2011

Keywords:

RAD001

Chloroquine

mTOR

p53

Breast cancer

ABSTRACT

PI3K/Akt/mTOR and p53 signaling pathways are frequently deregulated in tumors. The anticancer drug RAD001 (everolimus) is a known mTOR-inhibitor, but mTOR-inhibition leads to phosphorylation of Akt inducing resistance against RAD001 treatment. There is growing evidence that conflicting signals transduced by the oncogene Akt and the tumorsuppressor p53 are integrated via negative feedback between the two pathways. We previously showed that the anti-malarial Chloroquine, a 4-alkylamino substituted quinoline, is a p53 activator and reduced the incidence of breast tumors in animal models. Additionally, Chloroquine is an effective chemosensitizer when used in combination with PI3K/Akt inhibitors but the mechanism is unknown. Therefore, our aim was to test, if Chloroquine could inhibit tumor growth and prevent RAD001-induced Akt activation.

Chloroquine and RAD001 caused G1 cell cycle arrest in luminal MCF7 but not in mesenchymal MDA-MB-231 breast cancer cells, they significantly reduced MCF7 cell proliferation on a collagen matrix and mammospheroid formation. In a murine MCF7 xenograft model, combined treatment of Chloroquine and RAD001 significantly reduced mammary tumor growth by 4.6-fold ($p = 0.0002$) compared to controls. Chloroquine and RAD001 inhibited phosphorylation of mTOR and its downstream target, S6K1. Furthermore, Chloroquine was able to block the RAD001-induced phosphorylation of Akt serine 473.

The Chloroquine effect of overcoming the RAD001-induced activation of the oncogene Akt, as well as the promising antitumor activity in our mammary tumor animal model present Chloroquine as an interesting combination partner for the mTOR-inhibitor RAD001.

© 2011 Elsevier Inc. All rights reserved.

* Corresponding author. Tel.: +49 9131 8533553.

E-mail addresses: christian.loehberg@uk-erlangen.de (C.R. Loehberg), pamela.strissel@uk-erlangen.de (P.L. Strissel), ralf.dittrich@uk-erlangen.de (R. Dittrich), reiner.strick@uk-erlangen.de (R. Strick), juergen.dittmer@medizin.uni-halle.de (J. Dittmer), angeladittmer@yahoo.de (A. Dittmer), ben.fabry@biomed.uni-erlangen.de (B. Fabry), willi.kalender@imp.uni-erlangen.de (W.A. Kalender), thorsten.koch@biomed.uni-erlangen.de (T. Koch), david.wachter@uk-erlangen.de (D.L. Wachter), nicole.groh@gmx.de (N. Groh), astrid.polier@uk-erlangen.de (A. Polier), ina.brandt@gmx.de (I. Brandt), laura.lotz@uk-erlangen.de (L. Lotz), inge.hoffmann@uk-erlangen.de (I. Hoffmann), florentine.koppitz@uk-erlangen.de (F. Koppitz), sonja.oeser@uk-erlangen.de (S. Oeser), andreas.mueller@uk-erlangen.de (A. Mueller), peter.fasching@uk-erlangen.de (P.A. Fasching), michael.lux@uk-erlangen.de (M.P. Lux), matthias.beckmann@uk-erlangen.de (M.W. Beckmann), michael.schrauder@uk-erlangen.de (M.G. Schrauder).

1. Introduction

The phosphatidylinositol 3-kinase (PI3K)/Akt/mTOR pathway plays an important role in the biology of human cancers. Components of this pathway are frequently deregulated in a wide range of tumors, making them an attractive target for cancer therapy. The mammalian target of the drug rapamycin (mTOR) belongs to the PI3K related family of protein kinases [1] and is activated by phosphorylation at serine 2448 (S2448) [2]. In mammalian cells mTOR is part of two different kinase complexes, mTORC1 composed of mTOR, raptor and mLST8, and mTORC2 containing mTOR, rictor, Sin1 and mLST8. Whereas, mTORC1 is known to be a pivotal regulator of cell size and cell cycle control, the question whether the recently discovered mTORC2 complex is involved in these processes remained elusive [3,4]. The best characterized downstream effectors of mTORC1 are the ribosomal

S6 kinase 1 (S6K1) and the eukaryotic translation initiation factor 4E binding protein 1 (4E-BP1) [3], both regulators of mRNA translation. The activity of S6K1 is controlled by multiple phosphorylation events located within the catalytic, linker and pseudosubstrate domains [5,6]. Drug mediated mTORC1 inhibition can also induce phosphorylation of the oncogene Akt in various cancer cell lines and patient tumors [7–10], which may result in an attenuated treatment response [4].

RAD001 (everolimus) is a rapamycin-derivative and macrolide formulated for oral administration, which has been developed as an anti-proliferative drug with applications as an immune suppressant and anticancer agent [11,12]. RAD001 acts by selectively inhibiting mTORC1 (mTOR/raptor) [7,10,13,14] and holds promise as a therapeutic agent because of its low toxicity and its effects even at nanomolar concentrations. Although mTORC1 inhibition by rapamycin or RAD001 leads to activation and phosphorylation of Akt at the crucial phosphorylation site serine 473 [7–10] and is linked with reduced therapeutic effects [15], it is important to unravel how this phenomenon relates to the biological significance of Akt signaling [12]. In this respect, revealing new compounds which regulate signal transduction of PI3K/Akt/mTOR pathway members may have potential implications for signaling and treatment approaches [16].

In this study in addition to RAD001 we tested if the drug Chloroquine (CQ), a 4-alkylamino substituted quinoline family member, could influence inhibition of breast cancer growth through regulation of PI3K/Akt/mTOR signaling as well as determine its ability to overcome RAD001-induced Akt activation. We previously demonstrated that CQ activated p53 and its downstream target gene p21 in the non-tumorigenic mammary gland epithelial cell line MCF10A [17], and there is growing evidence that conflicting signals transduced by Akt and p53 are integrated via negative feedback between the p53 and the PI3K/Akt/mTOR signaling pathways [18,19]. Furthermore CQ was recently shown to act as an effective chemosensitizer when used in combination with PI3K/Akt inhibitors [20,21] and we could previously show its ability to exert specific breast cancer protective effects in an animal model [17].

This present study demonstrates that CQ specifically regulates members of the PI3K/Akt/mTOR and p53 signaling pathways. In a murine mammary tumor xenograft model we also demonstrate an additive suppression of tumor growth when mice were treated with CQ in combination with RAD001.

2. Material and methods

2.1. Cell culture

The human MCF7 (p53 wildtype, ER-positive, luminal cell) [22] and MDA-MB-231 (p53 mutated, ER-negative, mesenchymal) [23] breast cancer cell lines (all from ATCC, Promocell, Heidelberg, Germany) were cultured in Dulbecco's Modified Eagle's Medium (DMEM) supplemented with 10% fetal calf serum (FCS), nonessential amino acids, L-glutamine, and HEPES buffer (all from Invitrogen, Karlsruhe, Germany) at 37 °C with a 5% CO₂–95% air atmosphere. Cells were incubated in media in the presence of low growth factors and hormones (5% CTS) for 24 h prior to treatment with 50 μmol/l CQ (Sigma–Aldrich, Taufkirchen, Germany) and/or 20 nmol/l RAD001 (Novartis, Basel, Switzerland).

2.2. Flow cytometry

Cells were trypsinized into single-cell suspension, fixed in ice cold 70% ethanol, and stored at –20 °C. Before analysis, cells were resuspended in PBS (Invitrogen, Karlsruhe, Germany) with 500 μg/ml RNase A (Promega, Mannheim, Germany) at room temperature,

50 μg/ml propidium iodide (PI) (Sigma–Aldrich, Taufkirchen, Germany), according to standard protocols. Analysis was done on a Becton Dickinson fluorescence activated cell sorter (FACScan). Differences of cells after treatment were examined by two-sided *t*-test with *p* < 0.05 considered as statistically significant.

2.3. Collagen proliferation assays

Collagen beds containing calf skin type I collagen G (Serva Electrophoresis, Heidelberg, Germany) and rat tail type I collagen R (Biochrom AC, Berlin, Germany) along with culture media, sodium bicarbonate, and sodium hydroxide (all Invitrogen, Karlsruhe, Germany) were plated into tissue culture wells of 11.04 cm² according to Wacker et al. [24]. To assess cell proliferation 80,000 MCF7 breast cancer cells were seeded on top of each collagen bed per well in DMEM media with 10% CTS. Proliferation cell counts were performed following fixation with 2.5% glutaraldehyde (Sigma–Aldrich, Taufkirchen, Germany) at day 1 (24 h after cell attachment with no drugs) then drugs were added and further counted at day 3 (72 h), day 5 (120 h) and day 7 (168 h). The media was renewed a second time at 96 h with or without drugs. Prior to analysis all cells were stained with Hoechst 33568 (1.7 μg/ml) (Sigma–Aldrich, Taufkirchen, Germany) in PBS.

As MCF7 cells tend to cluster in small three-dimensional (3D) colonies when grown on 3D collagen gels, counting individual nuclei is difficult and prone to error. To quantify proliferation of MCF7 cells following drug treatment, we implemented a method based on the following idea: We reasoned that, with all experimental conditions being constant, the average fluorescence intensity obtained from a given image or field-of-view represented a measure of the DNA stained with Hoechst dye. Using a motorized Epi-fluorescence microscopy equipped with a 10x objective (Leica, Wetzlar, Germany) we focused to the top of the collagen gel and acquired images at 49 random locations. After subtracting the background intensity, the average fluorescence intensity was taken as a measure of DNA amount [25]. Statistical analysis (PASW statistics 18.0) was performed using the Wilcoxon rank-sum test with *p* < 0.05 considered as statistically significant.

2.4. Three-dimensional breast cancer cell mammospheroid model

MCF7 cells were grown in 3D cultures as previously described [26,27]. Briefly, cells were trypsinized and grown on top of a layer of 2% Seakem GTG agarose (ViaLight Plus, Lonza, Rockland, USA) (dissolved in PBS) without the addition of matrix proteins. The freely floating MCF7 cells aggregated to form colonies and then developed into mammospheroids within 2–3 days. CQ and/or RAD001 were added before and after mammospheroid formation (CQ (50 μM), RAD001 (20 nM)) for a total incubation time of 3 days. Cellular ATP levels were measured to determine the number of viable cells (ViaLight Plus, Lonza, Rockland, USA). Differences in the fraction of surviving cells after treatment were examined by two-sided *t*-test with *p* < 0.05 considered as statistically significant.

2.5. MCF7 Xenograft nude mouse model

We established a murine breast cancer model with MCF7 breast cancer cells. Following exponential growth in cell culture and harvesting, MCF7 breast cancer cells were resuspended in PBS. For the inoculations, MCF7 breast cancer cells were washed with PBS, trypsinized, pooled and resuspended in DMEM, then centrifuged and resuspended in 0.3 ml Matrigel/DMEM mix (4:1) (BD Matrigel, Basement Membrane Matrix, LDEV-Free, BD Biosciences, Erembodegem, Belgium), as previously described [28]. 5 × 10⁶ cells were injected into the fat pad of the 3rd and 4th inguinal mammary

glands of 4–6-week-old, female nude mice (NMRI nu/nu mice, Janvier, St. Berthevin Cedex, France).

All animals were housed according to approved German laboratory animal care guidelines under conditions of a 12-h light/dark cycle, and permitted ad libitum access to food and water. All experiments were performed in accordance with German protection of animal act and a valid license for animal testing (Reg.-Nr.: 54-2532.1-35/08) is existent.

For tumor growth of MCF7 breast cancer cells a supportive hormonal treatment was necessary and 17 β -estradiol pellets (0.72 mg, 60-day release, Innovative Research of America, Sarasota, Florida, USA) were implanted s.c. in the interscapular region to create constitutive high hormone levels for tumor growth [22]. Mice were treated with RAD001 alone (10 mg/kg, orally via gauge) 5 days a week (according to RAD001 Investigator's Brochure, Novartis Switzerland); with CQ alone (50 mg/kg, intraperitoneally) 3 days a week and modified according to several publications [17,29–31]; or with a combination of RAD001 and CQ ($n = 10$ for each treatment group). Tumor volume was measured in vivo with calipers and calculated (tumor volume = (length \times width²)/2). After animals were sacrificed tumors were measured by weight and by computer micro-tomography imaging in the Micro CT Tomoscope Duo (CT Imaging GmbH, Erlangen, Germany). Tumor volume was calculated from 3D CT images by summation over all voxels with intensity above a tumor-specific value. Differences of tumor growth after treatment were examined by two-sided t -test with $p < 0.05$ considered as statistically significant.

Hematoxylin/eosin (HE) staining of paraffin embedded xenograft tumors: At the Institute of Pathology (Erlangen, Germany) tumors were fixed in 10% formalin for 1 h, washed several times with ethanol (70–100%) for 5.5 h and xylol (2.5 h) and embedded into paraffin (2 h) (all SAV Liquid Production, Flintsbach, Germany). HE staining of 5 μ m tissue sections was performed by automation (Gemini, Shandon Varistain Slide Stainer, GMI Inc., USA) following deparaffinization with xylol for 10 min, washed with ethanol and water and then stained with hematoxylin gill #3 (3 min) and eosin (20 s) (all Sigma–Aldrich, Taufkirchen, Germany) and then analyzed for histology.

2.6. Immunohybridization analysis

Nuclear extracts were prepared with the NEPER lysis buffer kit (Pierce, Thermo Fisher Scientific, Bonn, Germany). For immunohybridization, the lysates were resolved by SDS-PAGE and transferred to a nitrocellulose membrane according to Strissel et al. [32]. The blots were hybridized with the following mono- or polyclonal antibodies (Ab) made in rabbits from Cell Signaling Technology (Life technologies, Darmstadt, Germany) to detect the human proteins: p-p53 (S15), 1:1000; p53,1:1000; p21, 1:1000; p-mTOR (S2448), 1:1000; mTOR, 1:1000; p-S6K1 (T389), 1:1000; S6K1, 1:1000; p-Akt (S473) (HRP Conjugate), 1:1000; Akt (pan), 1:1000. Nuclear proteins on Western blots were normalized to Actin using anti-Actin mouse mAb (Millipore, Schwalbach, Germany), 1:1000. Specific proteins were visualized with anti-rabbit or anti-mouse IgG coupled to horseradish peroxidase (Santa Cruz Biotechnology, Heidelberg, Germany), using the ECL Reagent (GE Healthcare, Freiburg, Germany) and with the following antibodies: anti-rabbit IgG HRP-linked, Cell Signaling Technology (Life technologies, Darmstadt, Germany), 1:1000; Anti-mouse HRP-linked (Millipore, Schwalbach, Germany), 1:50,000–1:100,000; Anti-mouse IgG HRP-linked Ab, Cell Signaling Technology (Life technologies, Darmstadt, Germany), 1:1000. Protein signal intensities were measured using ImageJ 1.43 using Java Web <http://rsbweb.nih.gov/ij/applets.html> to quantify protein amounts. All protein band pixels were first subtracted from the background then normalized to Actin.

3. Results

3.1. Chloroquine and RAD001 inhibited MCF7 breast cancer cell proliferation via G1 cell cycle arrest

Flow cytometry was performed to determine whether CQ and RAD001 affect the cell cycle in MCF7 (luminal, p53 wildtype) and MDA-MB-231 (mesenchymal, p53 mutated) breast cancer cells. The DNA content of propidium iodide-stained (PI) nuclei from untreated, CQ- and RAD001-treated cells was analyzed. As shown in Fig. 1, after 24 h (and 72 h, data not shown) of drug treatment the percentage of MCF7 cells in G1 phase was 50% in the control, 62% with CQ (50 μ M), 65% with RAD001 (20 nM) and 74% with CQ- and RAD001-treatment, while in MDA-MB-231 cells no significant change could be seen.

In respect of CQ, this is in alignment with our previously published data stating a p53-dependent induction of a G1 cell cycle arrest [17]. For RAD001 we confirmed recently published data by Dittmer and colleagues that showed reduced viability of luminal MCF7 cells after RAD001 treatment, but RAD001 failed to affect the viability of 2D- and 3D-cultured mesenchymal MDA-MB-231 cells [33].

3.2. Chloroquine and RAD001 inhibition of 3D-cultured MCF7 cell proliferation

In order to determine to which extent CQ alone or together with RAD001 could inhibit growth of luminal MCF7 cells, proliferation studies were performed where cells were grown for 7 days in the presence or absence of drugs on a collagen matrix (Fig. 2). Using 3D Epi-fluorescence microscopy implemented with automatized scanning of collagen gels, the relative amount of DNA from Hoechst-stained nuclei was calculated. This technique demonstrated a high sensitivity of detecting small fluctuations in the number of nuclei.

Results showed that treatment of cells with RAD001 or CQ alone led to a decrease in proliferation from days 3 to 7 between 45–58% and 20–37%, respectively, compared to controls which increased in proliferation till day 7. Importantly, an additive suppression of MCF7 cellular proliferation was noted between 45 and 71% when cells were treated with CQ in combination with RAD001 (Fig. 2).

3.3. Chloroquine and RAD001 reduced MCF7 mammospheroid formation in 3D-cell cultures

Dittmer and colleagues were able to show in a 3D cell culture model that MCF7 cells aggregate to form tumor mammospheroids that resemble the natural process of acinar formation during mammary gland morphogenesis [27]. Due to the ability of mammary cells to produce a cellular matrix, mammospheroid formation into 3D structures can also occur without the addition of an extracellular matrix in cell cultures. Therefore, we analyzed the effect of CQ and RAD001 on mammospheroid formation of MCF7 breast cancer cells in 3D cultures.

Results showed that untreated MCF7 cells formed mammospheroids in 3D cultures after 3 days (Fig. 3). In contrast, all drug combinations of CQ and RAD001 treatment of cells showed a reduction of mammospheroid formation (CQ 18%, RAD001 20%) by measuring the number of viable cells based on ATP cellular levels (Fig. 3A). Importantly, additive inhibitory effects were seen when both drugs were administered in combination in cell cultures when compared to single drug treatments (CQ and RAD001 37%, $p < 0.05$). In addition, further microscopic analyses demonstrated that the mock- and RAD001-treated mammospheroids generally appeared more translucent (Fig. 3B). In contrast, CQ-treated mammospheroids showed microscopically more compact and less translucent mammospheroid architecture with an irregular surface (Fig. 3B).

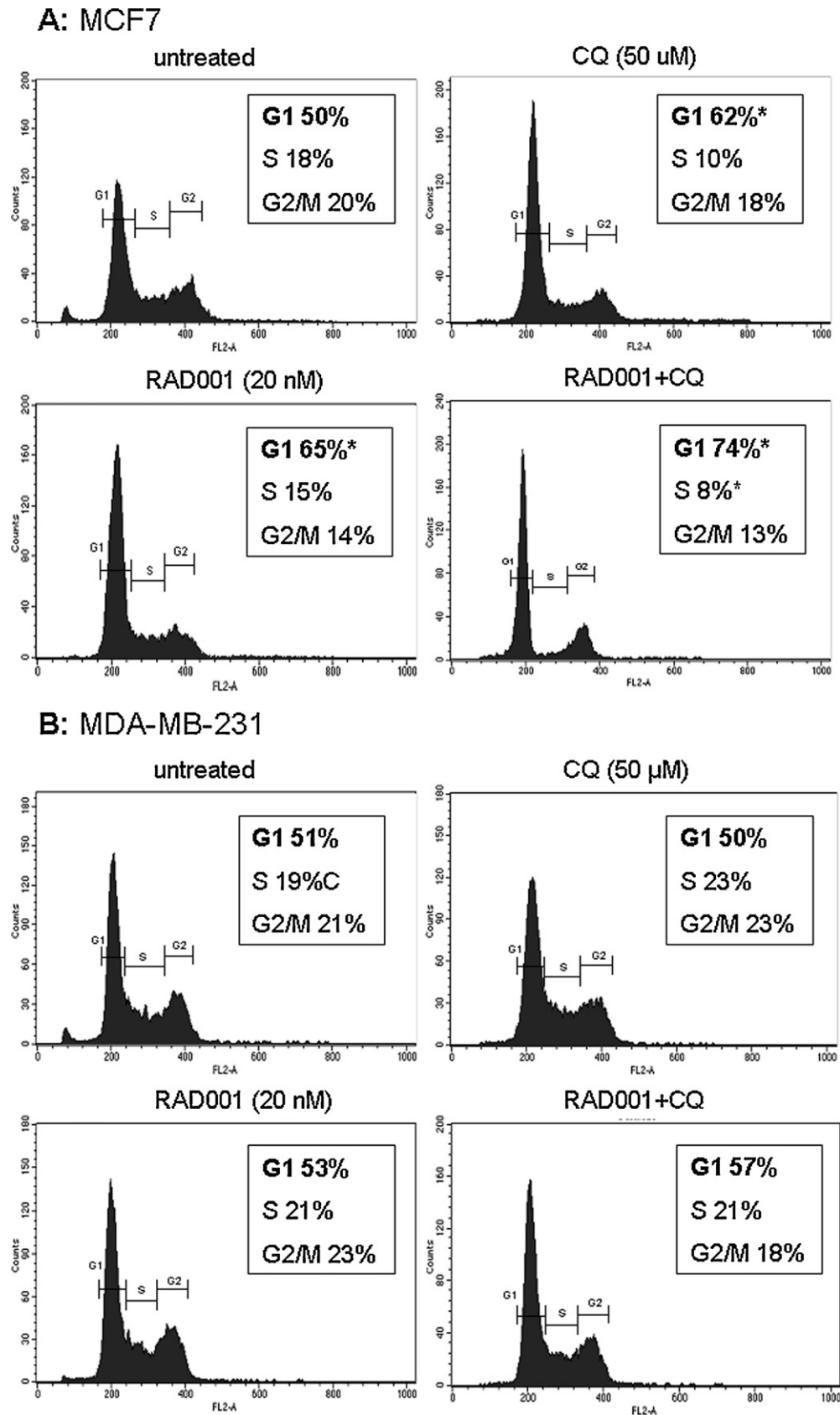


Fig. 1. Induction of a G1 cell cycle arrest in luminal MCF7 breast cancer cells, but not in mesenchymal MDA-MB-231 breast cancer cells. The DNA content of propidium iodide-stained (P.I.) nuclei from untreated, CQ- and RAD001-treated cells were analyzed by FACS. (A) The percentage of MCF7 cells in the G1 phase was 50% in the control, 62% with CQ (50 μ M), 65% with RAD001 (20 nM) and 74% with CQ- and RAD001-treatment after 24 h (and 72 h, data not shown), (B) no changes were seen in MDA-MB-231 cells. All experiments were performed in triplicate and (*) for statistically significance values $p < 0.05$.

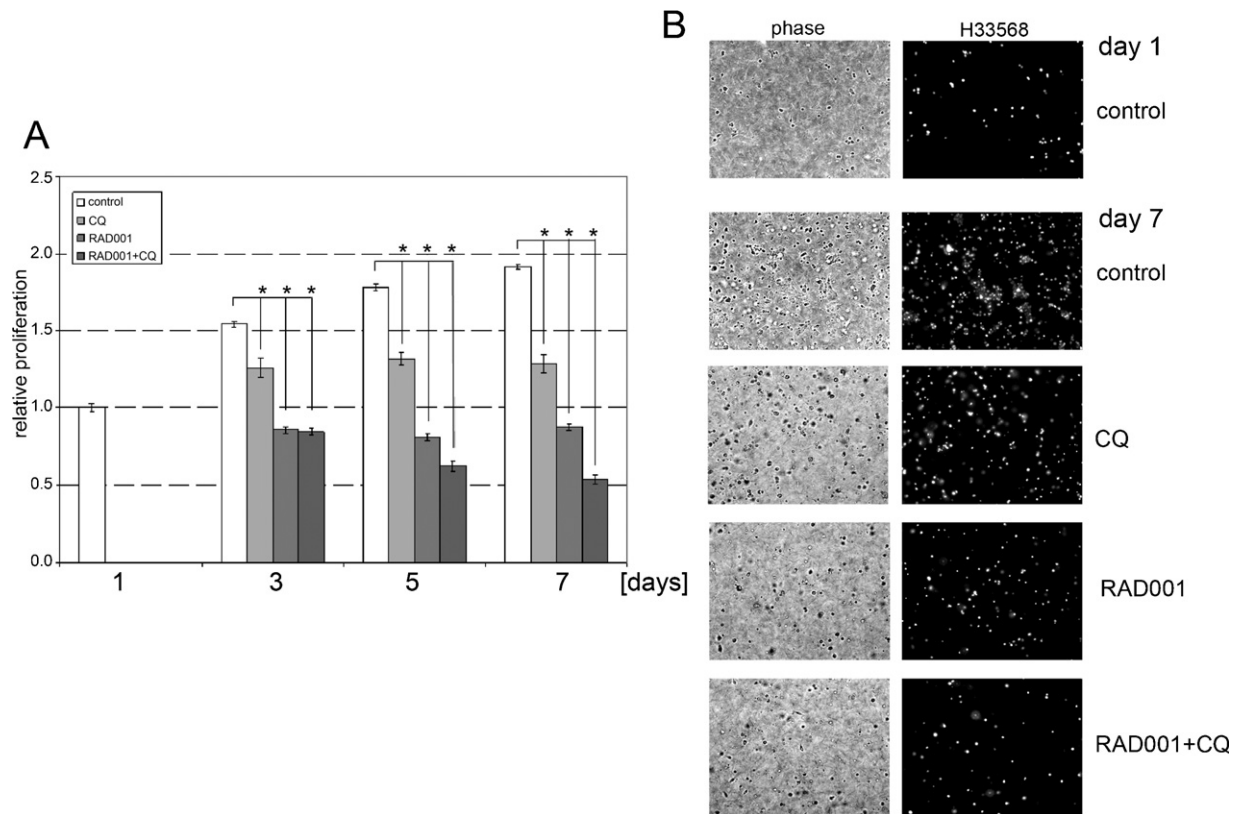


Fig. 2. Inhibition of MCF7 breast cancer cell proliferation in a 3D cell culture by CQ and RAD001. (A) MCF7 breast cancer cells were grown on collagen in the presence of CQ (50 μM), RAD001 (20 nM) and CQ + RAD001 in combination for 7 days. Graph represents the mean-fold increase of cellular proliferation for untreated cells and the mean-fold decrease after drug treatment. All experiments were performed in triplicate. Standard deviation is shown and (*) for statistically significance values $p < 0.001$. Mean-fold values representing the total nuclear area in μm^2 are the following: day 1 untreated = $39,577 \pm 950$; day 3 untreated = $60,982 \pm 1025$, CQ = $49,720 \pm 3044$, RAD001 = $34,043 \pm 715$, CQ + RAD001 = $33,637 \pm 681$; day 5 untreated = $70,442 \pm 1557$, CQ = $52,103 \pm 2086$, RAD001 = $32,207 \pm 776$, CQ + RAD001 = $24,717 \pm 849$; day 7 untreated = $75,881 \pm 1168$, CQ = $50,897 \pm 2831$, RAD001 = $34,610 \pm 608$, CQ + RAD001 = $21,333 \pm 635$. (B) Phase contrast and matching Hoechst 33568 stained nuclei were quantified (total nuclear area in μm^2) using 3D Epi-fluorescence microscopy to determine the relative level of cellular proliferation as shown in (A).

3.4. Antitumor activity of Chloroquine and RAD001 in a mammary MCF7 xenograft nude mouse model

To further evaluate CQ and RAD001 inhibition of tumor growth, we established a human mammary MCF7 xenograft nude mouse

model. Therefore, we tested the effects of combined CQ and RAD001 treatment in our MCF7 breast cancer xenograft nude mouse model. Throughout the time period of 28 days, both CQ and RAD001 treatment of mice resulted in a reduction of tumor size compared to control mice (Fig. 4). After animals were sacrificed at

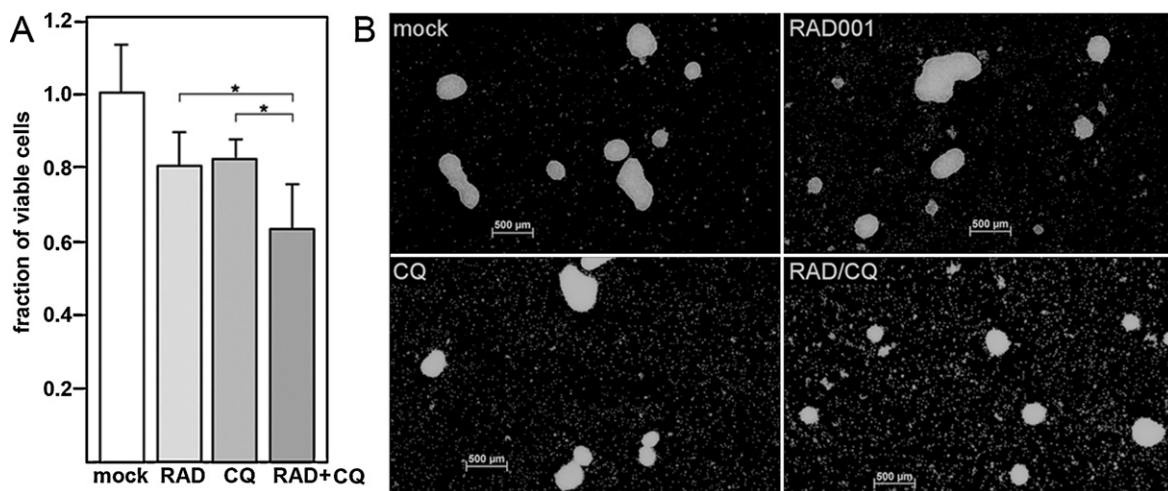


Fig. 3. CQ and RAD001 reduced MCF7 mammospheroid formation in 3D cell cultures. (A) MCF7 cells formed mammospheroids in 3D cell cultures. The graph shows the fraction of viable cells of mammospheroids by measuring ATP cellular levels following CQ and/or RAD001 addition to MCF7 3D cell cultures before and after spheroid formation (CQ = 50 μM , RAD001 = 20 nM) ($N = 6$). Mock = 1.0 ± 0.13 ; RAD001 (RAD) = 0.8 ± 0.09 ; CQ = 0.82 ± 0.05 ; RAD001 + CQ = 0.63 ± 0.12 . Note that a statistically significant reduction of spheroid formation occurred in 3D cell cultures treated with the drug combination ($*p < 0.05$). (B) Microscopy pictures demonstrate less spheroid formation and more single cells in drug treated groups. Note the more compact and less translucent mammospheroid architecture with an irregular surface structure after 3 days of CQ drug treatment.

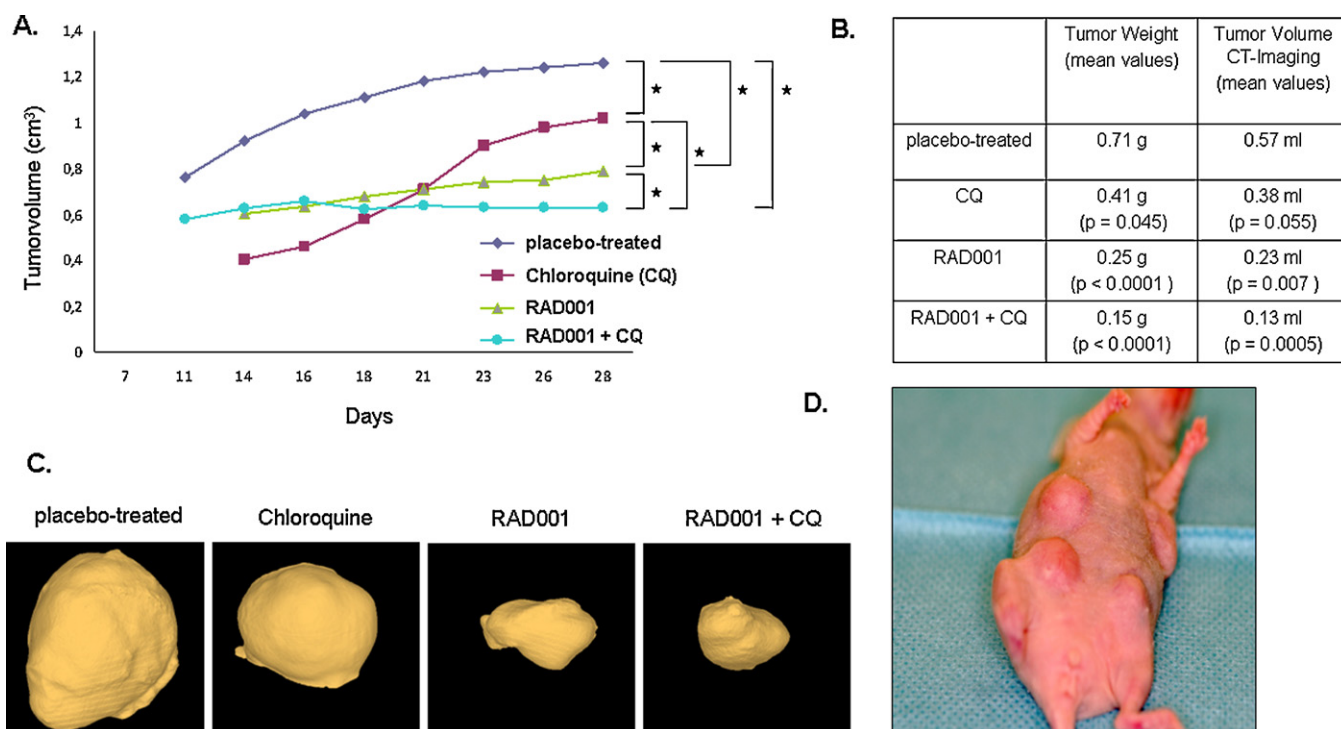


Fig. 4. Inhibition of tumor growth in the human mammary MCF7 xenograft nude mouse model after treatment with CQ and RAD001. After injection of MCF7 breast cancer cells into the inguinal mammary glands, female nude mice were treated with RAD001 alone (10 mg/kg), with CQ (50 mg/kg) alone, or with a combination of RAD001 and CQ ($n = 10$ for each treatment group). (A) As represented on the graph, tumor growth measurements were followed from 7 to 28 days as tumor volume (cm^3). (B) Tumor measurements after resection of sacrificed animals. (C) Tumors isolated at day 28 from CQ, RAD001 and RAD001 and CQ treated mice are shown as 3D images using computer micro-tomography. (D) Photo of a single control mouse at day 28 with inguinal mammary gland tumors. Asterisk (*) for statistically significance values $p < 0.05$.

day 28, tumors were further measured by weight and by computer tomography imaging. Compared to tumors from control mice, RAD001-treated mice demonstrated tumors which were 2.9-fold lighter ($p < 0.0001$) and 3.3-fold smaller ($p < 0.0001$) whereas CQ-treated mice showed tumors which were only 1.7-fold lighter ($p = 0.005$) and 1.6-fold smaller ($p = 0.01$). However, tumors treated with RAD001 plus CQ were 4.1-fold lighter ($p < 0.0001$) and nearly 4.6-fold smaller ($p = 0.0002$) than control mice.

A further analysis was performed to determine tumor histology. Hematoxylin and eosin staining of all xenograft tumors confirmed an invasive ductal adenocarcinoma mammary tumor phenotype (data not shown). It is important to note that mice treated with RAD001 were more effective in reduction of these tumors than with CQ. Additionally, CQ and RAD001 in combination provided an additive benefit for reduction of tumor growth.

3.5. Chloroquine leads to p53-activation and reduces RAD001-induced increase of Akt phosphorylation

Since we previously determined that CQ induced p53 in MCF10A breast epithelial cells [17], we tested the effect of CQ and RAD001 on this protein in nuclear extracts from MCF7 breast cancer cells. To determine whether CQ-induced cell cycle arrest is associated with up-regulation of the p53-dependent cell cycle inhibitor p21 (Waf1/Cip1) [34], we also examined the levels of the p21 protein after CQ treatment. p21 plays a significant role in cell cycle arrest via enforcing G1 restriction point by inhibitory binding to cdk2/cyclin E or other cdk/cyclin complexes [34]. Results showed that both p53 and p21 levels increased following treatment of MCF7 cells with CQ, but not RAD001 (Fig. 5). Furthermore we could show increased phosphorylation of the crucial phosphorylation site serine 15 by treatment with CQ. Thus, our data supports that the G1 cell cycle arrest induced by CQ was mediated by p53 and p21.

We further sought to determine whether the RAD001-induced increase of Akt phosphorylation at the crucial phosphorylation site serine 473 could be modified [7–10]. Thus, we tested the effect of CQ, on the RAD001-mediated feedback activation of Akt signaling. As shown in Fig. 5, treatment of MCF7 cells with CQ resulted in a reduction of RAD001-induced increase of Akt phosphorylation at serine 473.

mTOR is phosphorylated at serine 2448 via the IGF-1/PI3K/Akt signaling pathway [2,35]. We could confirm the mTOR-inhibitory effect by RAD001 showing a lucid reduction in phosphorylation at serine 2448 in MCF7 cells, which was also seen to a lesser extent by CQ treatment, and in combination of RAD001 and CQ phosphorylation of mTOR at serine 2448 was even further decreased, see Fig. 5.

The mTOR downstream target gene S6K1 has two known isoforms, p70S6K1 and p85S6K1 [36], which both are detected by antibodies used in immunohybridization. p85S6K1 is derived from the same gene and is identical to p70S6K1 except for 23 extra residues at the amino terminus, which encode a nuclear localizing signal [36]. p70S6K1 phosphorylation of threonine 389, however, most closely correlates with S6K1 activity [5,6]. Examining p70S6K1 revealed a decrease in phosphorylation levels at this crucial site confirming a reduced activity of this mTOR downstream target gene.

These data suggest that CQ might exert at least parts of its anti-cancer effects through modifications of the IGF-1/PI3K/Akt/mTOR and p53 pathways.

4. Discussion

Tumors exhibiting mutational activation of PI3K, a common event in cancers, are hypersensitive to mTOR inhibitors like rapamycin and RAD001 [8]. Targeting breast cancer with RAD001 has led to significant improvements in treatment [7,10,37].

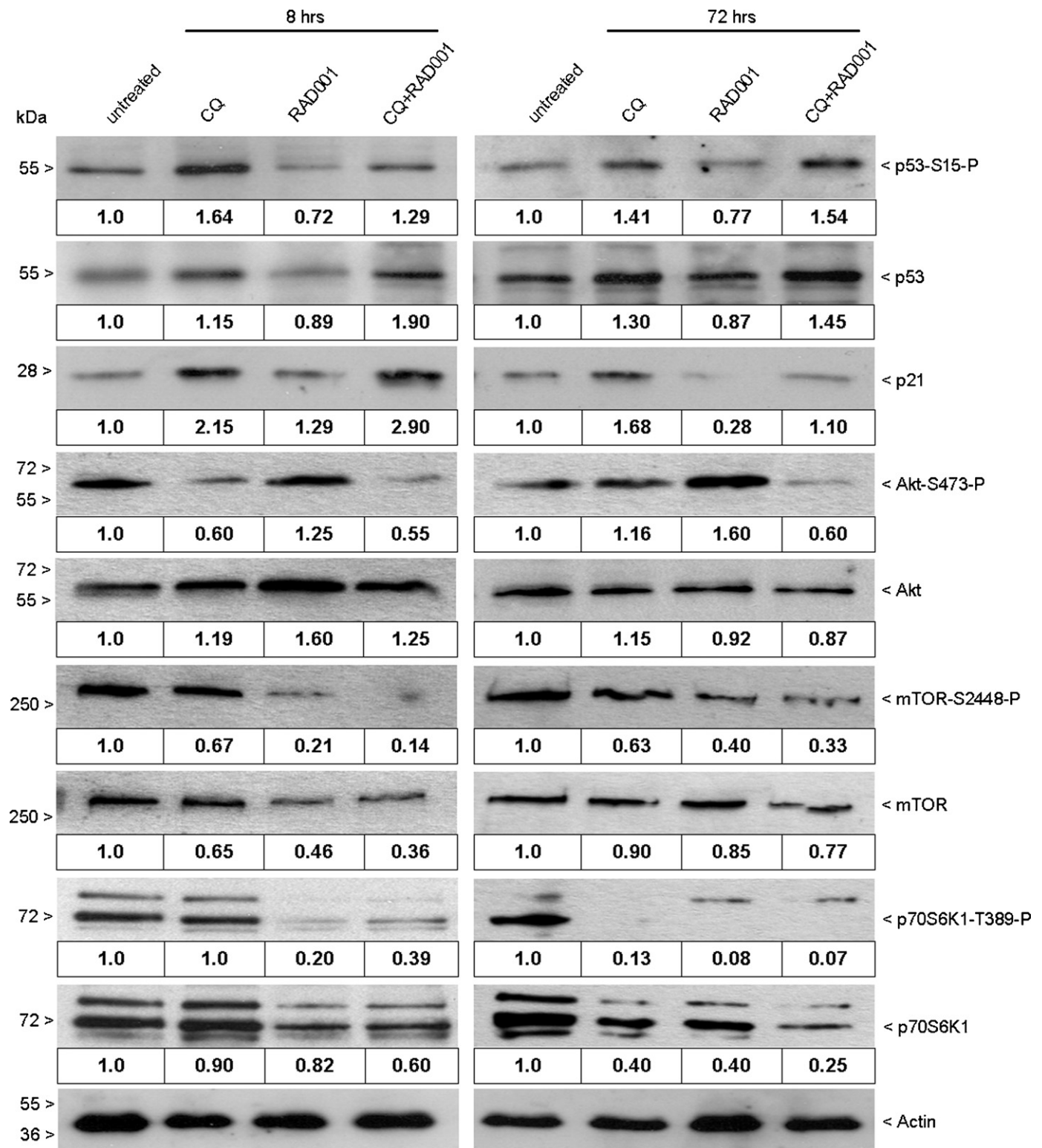


Fig. 5. Immunohybridization of PI3K/mTOR/Akt- and p53-signaling members in MCF7 nuclear cell lysates following treatment with RAD001 and CQ. Protein lysates with matching protein quantification of the PI3K/Akt/mTOR and p53 signaling members are shown after CQ (50 μ M) and RAD001 (20 nM) cell treatment at the indicated time points. Both total and phosphorylated proteins of signaling members are indicated on the right. All proteins were normalized to Actin. All experiments were performed in triplicate.

However, in advanced disease, mTOR inhibitors lose their efficiency due to drug resistance [38]. Therefore, understanding the mechanisms leading to resistance of mTOR inhibitors may eventually guide development of successful mTOR-targeted cancer therapy. In this investigation, our main interest was to determine whether mTOR inhibition by RAD001 in combination with CQ

results in enhanced inhibition of mammary tumor growth and could differentially regulate members of the PI3K/mTOR/Akt signaling pathway. In addition, we support the hypothesis that prolonged RAD001-induced Akt activation leads to drug resistance. Therefore we tested, if CQ could modulate the RAD001-induced Akt activation in MCF7 cells.

Previously, a negative feedback loop was described, whereby mTOR/S6K1 activation attenuated PI3K signaling by suppressing the function of the insulin receptor substrate-1 (IRS1), a mediator of insulin receptor-dependent activation of PI3K [8]. This data suggested that feedback down-regulation of receptor tyrosine kinase signaling was a frequent event in tumor cells with constitutive mTOR activation [8]. On the other hand, it was shown that mTOR inhibition by RAD001 could induce expression of IRS1 and abrogate feedback inhibition of the pathway, resulting in Akt activation in tumor cells [7–10]. In this report we could corroborate the mTOR-inhibitory effect of RAD001 [13,14] by showing reduced phosphorylation at serine 2448 of mTOR in MCF7 cells.

There is growing evidence that conflicting signals transduced by Akt and p53 are integrated via negative feedback between the PI3K/Akt/mTOR and p53 signaling pathways [18,19]. It has been suggested that depending on the balance of signals, p53-dependent downregulation of Akt may promote an irreversible commitment to apoptotic cell death, whereas effective recruitment of Akt by appropriate survival signals may lead to inactivation of p53, and eventually to inhibition of p53-dependent apoptosis and cell cycle arrest [18,19]. On the other side, p53 can be activated by several PI3K-related kinases (PIKK), including ataxia telangiectasia mutated (ATM), ATM- and Rad3-related (ATR); and the ATM downstream effector checkpoint kinases Chk1 or Chk2 that phosphorylate the NH2 terminal transactivation domain of p53 at multiple sites (e.g., serines 6, 9, 15, 20, 37, and 46; Refs. [39–43]).

In an attempt to improve RAD001 treatment and overcome RAD001-induced activation of the oncogene Akt, we focused our studies on this approach and the p53-activator CQ [17]. CQ is also a known inhibitor of lysosomal enzyme activity [44] and recent studies draw interest on this feature [45]. At low doses CQ is able to alter chromatin and chromosome structures in the absence of DNA breaks, but the mechanism of these modifications is only partially understood [46–49]. Importantly, we previously showed that CQ activates the ATM protein and causes both phosphorylation of p53 at serine 15 and auto-phosphorylation of ATM at serine 1981 in mammary epithelial cells at doses with low cytotoxicity and no significant inhibition of autophagy nor DNA-breakage [17]. In our current study we showed CQ-induced up-regulation of p53 and p21, the key players for G1 cell cycle arrest, in the MCF7 breast cancer cells, we were able to achieve a reduced RAD001-induced Akt activity by co-treatment with CQ, and could furthermore describe an mTOR-inhibitory effect of CQ.

Absence of CQ- and RAD001-induced G1 cell cycle arrest in p53-mutated, mesenchymal MDA-MB-231 breast cancer cells indicates a possible p53-dependency of CQ's inhibitory activity. This is in alignment with our previously published data [17] reporting that CQ significantly reduced the incidence of N-methyl-N-nitrosourea-induced mammary tumors in an animal model, but no protection was seen in a BALB/c p53-null mammary epithelium model, indicating a p53 dependency for the CQ effect [17].

RAD001 has also been shown to have antitumor activity in human breast cancer xenograft models [50,51], to further evaluate the effectiveness of CQ and RAD001 we determined that especially the combination of CQ and RAD001 led to additive inhibition of tumor cellular growth in an animal model. Previous studies have indicated that although CQ does not show many side effects during long-term use for treatment of malaria or rheumatoid diseases, retinal problems are a potential side effect [52]. Based on the ophthalmologic safety guidelines for long-term use of CQ in humans [52] and on our previously published data [17], we chose the applied doses of CQ in our animal model for possible further clinical use. Therefore, our result of CQ-induced protection against mammary carcinogenesis at such low levels is highly significant and promising.

MCF7 collagen growth and formation of mammospheres along with FACS analyses supported that CQ and RAD001 induced growth inhibition via a G1 cell cycle arrest, where the CQ mediated cell cycle arrest involved phosphorylation of p53 and p21. In 3D cultures, breast cancer cells aggregate to form either tumor spheroids that resemble mammospheres of normal breast epithelial cells [53] or amorphous aggregates [26]. MCF7 spheroids show characteristics of an epithelium with apical tight junctions and desmosomes [54]. Like spheroids derived from immortalized nontumorigenic MCF10 breast epithelial cell spheroids [55], MCF7 spheroids develop a lumen after 7–10 days of culture [27]. We could not only demonstrate suppression of MCF7 cell proliferation by CQ in combination with RAD001 in a 3D cell culture, but our study revealed that both CQ and RAD001 disturb the architecture of the MCF7 mammary spheroid formation. These findings could also help to explain the antitumor effect we observed in our MCF7 xenograft nude mouse model.

All of the above results have several potential implications for the treatment of breast cancer with PI3K/Akt/mTOR pathway inhibitors. Another study demonstrated that mTOR inhibition by RAD001 was tightly associated with the development of drug resistance due to sustained Akt activation in lung cancer cell lines [15]. In the same study the authors demonstrated that by co-targeting mTOR and PI3K/Akt signaling with separate drugs resulted in blocking Akt phosphorylation and enhanced antitumor effects. Therefore, preventing Akt phosphorylation appears to be a key for successful mTOR-inhibitory drug therapy. It will be important to determine in future experiments if this mechanism is sufficient to prevent RAD001 drug resistance. It is clear that both our study and previously published investigations highly support CQ's ability to inhibit tumor growth especially in concert with other drugs. For example, treatment of several mammary cell lines in cell culture with CQ in combination with eleven different PI3K/Akt inhibitors demonstrated increased cell death up to 16.65-fold [20]. This study provided evidence that CQ represents a potent chemosensitizer in conjunction with a broad spectrum of drugs [20].

Taken together, our data support that the quinoline CQ exerts at least parts of its anti-cancer effects through modifications of the PI3K/Akt/mTOR pathway. The CQ effect of overriding the nuclear RAD001-induced Akt-phosphorylation, as well as its direct anti-tumor activity in our mammary tumor animal model present CQ as a promising combination partner of the mTOR-inhibitor RAD001.

Acknowledgments

This project was funded by the Deutsche Krebshilfe (108712) and a grant from the ELAN-Program (University of Erlangen) (07.03.16.2).

References

- [1] Keith CT, Schreiber SL. PIK-related kinases: DNA repair, recombination, and cell cycle checkpoints. *Science* 1995;270:50–1.
- [2] Schmelzle T, Hall MN. TOR, a central controller of cell growth. *Cell* 2000;103:253–62.
- [3] Bjornsti MA, Houghton PJ. The TOR pathway: a target for cancer therapy. *Nat Rev Cancer* 2004;4:335–48.
- [4] Shaw RJ, Cantley LC. Ras, PI(3)K and mTOR signalling controls tumour cell growth. *Nature* 2006;441:424–30.
- [5] Pullen N, Thomas G. The modular phosphorylation and activation of p70s6k. *FEBS Lett* 1997;410:78–82.
- [6] Weng QP, Kozlowski M, Belham C, Zhang A, Comb MJ, Avruch J. Regulation of the p70 S6 kinase by phosphorylation in vivo. Analysis using site-specific anti-phosphopeptide antibodies. *J Biol Chem* 1998;273:16621–9.
- [7] O'Donnell A, Faivre S, Burris 3rd HA, Rea D, Papadimitrakopoulou V, Shand N, et al. Phase I pharmacokinetic and pharmacodynamic study of the oral mammalian target of rapamycin inhibitor everolimus in patients with advanced solid tumors. *J Clin Oncol* 2008;26:1588–95.

- [8] O'Reilly KE, Rojo F, She QB, Solit D, Mills GB, Smith D, et al. mTOR inhibition induces upstream receptor tyrosine kinase signaling and activates Akt. *Cancer Res* 2006;66:1500–8.
- [9] Sun SY, Rosenberg LM, Wang X, Zhou Z, Yue P, Fu H, et al. Activation of Akt and eIF4E survival pathways by rapamycin-mediated mammalian target of rapamycin inhibition. *Cancer Res* 2005;65:7052–8.
- [10] Tabernero J, Rojo F, Calvo E, Burris H, Judson I, Hazell K, et al. Dose- and schedule-dependent inhibition of the mammalian target of rapamycin pathway with everolimus: a phase I tumor pharmacodynamic study in patients with advanced solid tumors. *J Clin Oncol* 2008;26:1603–10.
- [11] Huang S, Houghton PJ. Targeting mTOR signaling for cancer therapy. *Curr Opin Pharmacol* 2003;3:371–7.
- [12] Wan X, Harkavy B, Shen N, Grohar P, Helman LJ. Rapamycin induces feedback activation of Akt signaling through an IGF-1R-dependent mechanism. *Oncogene* 2006.
- [13] Breuleux M, Klopfenstein M, Stephan C, Doughty CA, Barys L, Maira SM, et al. Increased AKT S473 phosphorylation after mTORC1 inhibition is rictor dependent and does not predict tumor cell response to PI3K/mTOR inhibition. *Mol Cancer Ther* 2009;8:742–53.
- [14] Martin DE, Hall MN. The expanding TOR signaling network. *Curr Opin Cell Biol* 2005;17:158–66.
- [15] Wang X, Yue P, Kim YA, Fu H, Khuri FR, Sun SY. Enhancing mammalian target of rapamycin (mTOR)-targeted cancer therapy by preventing mTOR/raptor inhibition-initiated, mTOR/rictor-independent Akt activation. *Cancer Res* 2008;68:7409–18.
- [16] Scheid MP, Parsons M, Woodgett JR. Phosphoinositide-dependent phosphorylation of PDK1 regulates nuclear translocation. *Mol Cell Biol* 2005;25:2347–63.
- [17] Loehberg CR, Thompson T, Kastan MB, Maclean KH, Edwards DG, Kittrell FS, et al. Ataxia telangiectasia-mutated and p53 are potential mediators of chloroquine-induced resistance to mammary carcinogenesis. *Cancer Res* 2007;67:12026–33.
- [18] Gottlieb TM, Leal JF, Seger R, Taya Y, Oren M. Cross-talk between Akt, p53 and Mdm2: possible implications for the regulation of apoptosis. *Oncogene* 2002;21:1299–303.
- [19] Ogawara Y, Kishishita S, Obata T, Isazawa Y, Suzuki T, Tanaka K, et al. Akt enhances Mdm2-mediated ubiquitination and degradation of p53. *J Biol Chem* 2002;277:21843–50.
- [20] Hu C, Solomon VR, Ulibarri G, Lee H. The efficacy and selectivity of tumor cell killing by Akt inhibitors are substantially increased by chloroquine. *Bioorg Med Chem* 2008;16:7888–93.
- [21] Hu C, Raja Solomon V, Cano P, Lee H. A 4-aminoquinoline derivative that markedly sensitizes tumor cell killing by Akt inhibitors with a minimum cytotoxicity to non-cancer cells. *Eur J Med Chem* 2010;45:705–9.
- [22] Shafee SM, Liotta LA. Formation of metastasis by human breast carcinoma cells (MCF-7) in nude mice. *Cancer Lett* 1980;11:81–7.
- [23] Runcnebaum IB, Nagarajan M, Bowman M, Soto D, Sukumar S. Mutations in p53 as potential molecular markers for human breast cancer. *Proc Natl Acad Sci USA* 1991;88:10657–61.
- [24] Wacker I, Sachs M, Knaup K, Wiesener M, Weiske J, Huber O, et al. Key role for activin B in cellular transformation after loss of the von Hippel-Lindau tumor suppressor. *Mol Cell Biol* 2009;29:1707–18.
- [25] Mierke CT, Kollmannsberger P, Zitterbart DP, Diez G, Koch TM, Marg S, et al. Vinculin facilitates cell invasion into three-dimensional collagen matrices. *J Biol Chem* 2010;285:13121–30.
- [26] Dittmer A, Schunke D, Dittmer J. PTHrP promotes homotypic aggregation of breast cancer cells in three-dimensional cultures. *Cancer Lett* 2008;260:56–61.
- [27] Dittmer A, Hohlfeld K, Lutzkendorf J, Muller LP, Dittmer J. Human mesenchymal stem cells induce E-cadherin degradation in breast carcinoma spheroids by activating ADAM10. *Cell Mol Life Sci* 2009;66:3053–65.
- [28] VanWeelden K, Flanagan L, Binderup L, Tenniswood M, Welsh J. Apoptotic regression of MCF-7 xenografts in nude mice treated with the vitamin D3 analog, EB1089. *Endocrinology* 1998;139:2102–10.
- [29] Degtyarev M, De Maziere A, Orr C, Lin J, Lee BB, Tien JY, et al. Akt inhibition promotes autophagy and sensitizes PTEN-null tumors to lysosomotropic agents. *J Cell Biol* 2008;183:101–16.
- [30] Fu L, Kim YA, Wang X, Wu X, Yue P, Lonial S, et al. Perifosine inhibits mammalian target of rapamycin signaling through facilitating degradation of major components in the mTOR axis and induces autophagy. *Cancer Res* 2009;69:8967–76.
- [31] Bellodi C, Lidonni MR, Hamilton A, Helgason GV, Soliera AR, Ronchetti M, et al. Targeting autophagy potentiates tyrosine kinase inhibitor-induced cell death in Philadelphia chromosome-positive cells, including primary CML stem cells. *J Clin Invest* 2009;119:1109–23.
- [32] Strissel PL, Ellmann S, Loprich E, Thiel F, Fasching PA, Stiegler E, et al. Early aberrant insulin-like growth factor signaling in the progression to endometrial carcinoma is augmented by tamoxifen. *Int J Cancer* 2008;123:2871–9.
- [33] Dittmer A, Fuchs A, Oerlecke I, Leyh B, Kaiser S, Martens JW, et al. Mesenchymal stem cells and carcinoma-associated fibroblasts sensitize breast cancer cells in 3D cultures to kinase inhibitors. *Int J Oncol* 2011;39:689–96.
- [34] Koff A, Ohtsuki M, Polyak K, Roberts JM, Massague J. Negative regulation of G1 in mammalian cells: inhibition of cyclin E-dependent kinase by TGF-beta. *Science* 1993;260:536–9.
- [35] Nave BT, Ouwens M, Withers DJ, Alessi DR, Shepherd PR. Mammalian target of rapamycin is a direct target for protein kinase B: identification of a convergence point for opposing effects of insulin and amino-acid deficiency on protein translation. *Biochem J* 1999;344(Pt 2):427–31.
- [36] Reinhard C, Thomas G, Kozma SC. A single gene encodes two isoforms of the p70 S6 kinase: activation upon mitogenic stimulation. *Proc Natl Acad Sci USA* 1992;89:4052–6.
- [37] Baselga J, Semiglazov V, van Dam P, Manikhas A, Bellet M, Mayordomo J, et al. Phase II randomized study of neoadjuvant everolimus plus letrozole compared with placebo plus letrozole in patients with estrogen receptor-positive breast cancer. *J Clin Oncol* 2009;27:2630–7.
- [38] Gluz O, Liedtke C, Nitz U, Harbeck N. Molekulare Mechanismen der Chemoresistenz und Möglichkeiten der Überwindung. *Geburtsh Frauenheilk* 2009;69:138–44.
- [39] Appella E, Anderson CW. Post-translational modifications and activation of p53 by genotoxic stresses. *Eur J Biochem* 2001;268:2764–72.
- [40] Abraham RT. Cell cycle checkpoint signaling through the ATM and ATR kinases. *Genes Dev* 2001;15:2177–96.
- [41] Kastan MB, Lim DS. The many substrates and functions of ATM. *Nat Rev Mol Cell Biol* 2000;1:179–86.
- [42] Sorensen CS, Syljuasen RG, Falck J, Schroeder T, Ronnstrand L, Khanna KK, et al. Chk1 regulates the S phase checkpoint by coupling the physiological turnover and ionizing radiation-induced accelerated proteolysis of Cdc25A. *Cancer Cell* 2003;3:247–58.
- [43] Falck J, Mailand N, Syljuasen RG, Bartek J, Lukas J. The ATM-Chk2-Cdc25A checkpoint pathway guards against radioresistant DNA synthesis. *Nature* 2001;410:842–7.
- [44] Fedorko ME, Hirsch JG, Cohn ZA. Autophagic vacuoles produced in vitro. II. Studies on the mechanism of formation of autophagic vacuoles produced by chloroquine. *J Cell Biol* 1968;38:392–402.
- [45] Janku F, McConkey DJ, Hong DS, Kurzrock R. Autophagy as a target for anticancer therapy. *Nat Rev Clin Oncol* 2011;8:528–39.
- [46] Meshnick SR. Chloroquine as intercalator: a hypothesis revived. *Parasitol Today* 1990;6:77–9.
- [47] Krajewski WA. Alterations in the internucleosomal DNA helical twist in chromatin of human erythroleukemia cells in vivo influences the chromatin higher-order folding. *FEBS Lett* 1995;361:149–52.
- [48] Krajewski WA. Effect of in vivo histone hyperacetylation on the state of chromatin fibers. *J Biomol Struct Dyn* 1999;16:1097–106.
- [49] Krajewski WA, Lagarkova MA, Sharova NP, Stolyarov SD, Ausio J. Analysis of chromatin structural transitions by means of intercalator dyes. *Dokl Biochem Biophys* 2001;378:150–2.
- [50] Lu CH, Wyszomierski SL, Tseng LM, Sun MH, Lan KH, Neal CL, et al. Preclinical testing of clinically applicable strategies for overcoming trastuzumab resistance caused by PTEN deficiency. *Clin Cancer Res* 2007;13:5883–8.
- [51] Torres-Arzayus MI, Yuan J, DellaGatta JL, Lane H, Kung AL, Brown M. Targeting the AIB1 oncogene through mammalian target of rapamycin inhibition in the mammary gland. *Cancer Res* 2006;66:11381–8.
- [52] Rynes RI. Antimalarial drugs in the treatment of rheumatological diseases. *Br J Rheumatol* 1997;36:799–805.
- [53] Dontu G, Abdallah WM, Foley JM, Jackson KW, Clarke MF, Kawamura MJ, et al. In vitro propagation and transcriptional profiling of human mammary stem/progenitor cells. *Genes Dev* 2003;17:1253–70.
- [54] dit Faute MA, Laurent L, Ploton D, Poupon MF, Jardillier JC, Bobichon H. Distinctive alterations of invasiveness, drug resistance and cell-cell organization in 3D-cultures of MCF-7, a human breast cancer cell line, and its multidrug resistant variant. *Clin Exp Metastasis* 2002;19:161–8.
- [55] Muthuswamy SK, Li D, Lelievre S, Bissell MJ, Brugge JS. ErbB2, but not ErbB1, reinitiates proliferation and induces luminal repopulation in epithelial acini. *Nat Cell Biol* 2001;3:785–92.